X-ray fluorescence microtomography on a SiC nuclear fuel shell

M. Naghedolfeizi, J.-S. Chung, and G.E. Ice
Oak Ridge National Laboratory, Metals and Ceramics Division, Oak Ridge, TN 37830 USA
W.B. Yun, Z. Cai, and B. Lai
Argonne National Laboratory, Advanced Photon Source, Argonne, IL 60439 USA

TRISO fuel particles, used in high-temperature gas-cooled reactors (HTGR) are composite structures with a nuclear fuel kernel surrounded by alternating layers designed to contain fission products and compensate for radiation damage. As shown in Figure 1, a typical fuel particle contains an inner kernel of nuclear fuel, a low-density buffer layer of pyrocarbon, a dense layer of pyrocarbon coating, an interlayer of SiC, and a dense outer layer of pyrocarbon. The fuel kernel size, the thickness of the various layers, and the overall size of the TRISO fuel particle can vary with the type of fuel kernel [1]. The SiC layer provides the primary barrier for both radioactive elements in the kernel and gaseous and metallic fission products.

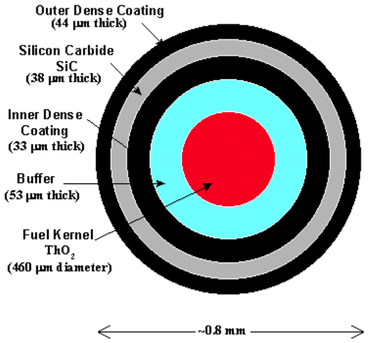

Figure 1: Schematic of TRISO fuel element.

X-ray fluorescence microtomography has been used to nondestructively measure trace elemental distribution in a SiC shell after exposure to a fluence of ~10^{25} (neutrons/m^2). The shell examined came from a previous study of diffusion through SiC shells [1] after the shells were exposed to varying fluences. The C buffer layers and nuclear kernels of the TRISO particles were removed by laser drilling through the SiC and then repeatedly leaching the particle in acid until a constant activity in the fission product was sensed [1]. At this point, it was assumed that any remaining activity was due to daughter products which had migrated into the SiC shell.

The experimental setup for an x-ray fluorescence tomography measurement is conceptually very simple. The sample is placed on a stage that rotates and translates the sample. A detector is placed in the plane of the storage ring at 90° to the incident beam to allow efficient measurement of the characteristic fluorescence from the trace elements and minimize the x-ray elastic and Compton scattering [3]. The elemental distribution in a slice through the sample can be reconstructed after translating the sample through the x-ray beam and rotating the sample at least 180° for every x position. Finer resolution is achieved by decreasing both the translation and rotational step size.

The experiment was performed on beamline 2-ID of the Advanced Photon Source [4]. Beamline 2-ID uses a low-bandpass x-ray mirror to define a beam axis followed by a Si(111) perfect crystal monochromator and a hard x-ray zone plate. The x-ray energy was set at 10.5 keV. For this experiment, a 40 cm focal length zone plate was used, which produced a spot size of approximately 1 x 3 µm^2. The sample was epoxied to a glass fiber and sandwiched between 2 mil Kapton tape to simplify handling. The fiber was mounted on a small goniometer head, which allowed the ball to be positioned at the center of rotation of the rotation stage. The ball was then centered on the x-ray beam so that the translation range of the measurement passed completely through the center of the ball.

Because a tomographic reconstruction requires consistent measurement conditions, the incident beam intensity was measured with an AMPTEC model XR-100T PIN diode detector with 250 eV energy resolution [5]. The detector was placed at ~90° 2θ to the beam but out of the plane of the x-ray ring (to optimize scattering efficiency). Scatter from the air between the sample and the zone plate was monitored. This crude incident beam monitor worked well after a backscatter shield was installed between the sample and the air volume viewed by the detector. Because of the limited beam time available, a compromised data collection scheme with 8 µm translation steps (101 translation steps) and 3° rotation steps (101 rotational steps) was used.

Before the tomographic measurements were begun, the unfocused beam was centered on the fuel ball shell to determine the detectable trace elements. Regions of interest (ROIs) were set around the dominant fluorescence lines (the K-lines of Ar, Ca, Cr, Fe, Ni, Cu, Zn and the L-line of Ba). Unfortunately, the Cs, Ce, and Eu L-lines lie in the region from 4.2 to 7 keV, substantially masked by intense K fluorescence from Cr and Fe. Therefore, with the solid-state detector, the distribution of the radioactive elements was not measured.

A single-line scan with 2 µm step size was then made to test the data collection software and hardware and to estimate typical feature sizes. There are numerous small Zn features through the shell, some of which are smaller than the 2 µm step resolution. The origin of this Zn is not known.

The absolute elemental concentrations were estimated by comparing the observed fluorescence signal ($S_{\text{Fluorescence}}$) to the x-ray elastic and Compton scattering signals. The total scattering cross section of SiC at 90° was estimated from [6]. The beam polarization was estimated at ~5% and multiple scattering and absorption were assumed to be small. With these approximations, the factor $I_0\Omega$ was determined, where I_0 is the incident beam flux in photons/sec/μm^2 and Ω is the detector solid angle. The trace element concentrations were then estimated again assuming negligible absorption from Equation 1:

$$S_{Fluorescence} \approx I_0\Omega\int\int\int\big(C(x,y,z)\sigma\big)dxdydz \quad (1)$$

Here C is the elemental concentration of the trace element and σ is the fluorescence cross-section at the incident beam energy. Self absorption in the sample was later corrected during the tomographic reconstruction. Tomographic reconstructions were carried out, both with and without absorption correction, using the library suite RECLBL [7]. However, prior to the image reconstruction phase, it was necessary to correct the scanned projection data for artifacts. This is because over a small angular range, the Kapton tape was at near glancing angle, which deflected and absorbed the incident beam. These conditions produced large artifacts in the data which were removed by excluding the data points from a small angular range and averaging neighboring data points to estimate the fluorescence intensities in the missing region. Of the 10^4 data points for each ROI, ~25 were corrected for the effect of the Kapton film. In addition, during the measurements, the detector was occasionally saturated by a huge fluorescence signal from unusually high concentrations of one or more trace elements. Under these conditions, the ROIs from all the elements were affected. The elements responsible were identified by observing the angle/translation pattern of each element and comparing them to the intense signal position. Approximately 20 points for each ROI were corrected for saturation effects using average neighboring data points. After correcting the artifacts, the Fourier filtered backprojection routine of the library was incorporated into a computer program, which reconstructed the two-dimensional images of the trace elements. The mode of reconstruction was based on 360° rotations and the choice of filter was Hannig with a cutoff frequency of 0.25. Because the reconstruction with 360° rotations appeared more robust, the missing 60° data was estimated from the 180° symmetric data.

The reconstructed spatial distributions of the monitored elements with absorption correction are presented in Figure 2. Although the fuel ball shell is only ~38 μm thick, absorption corrections can be large, particularly for the low-energy fluorescence lines. For example, ~97% of the Ba

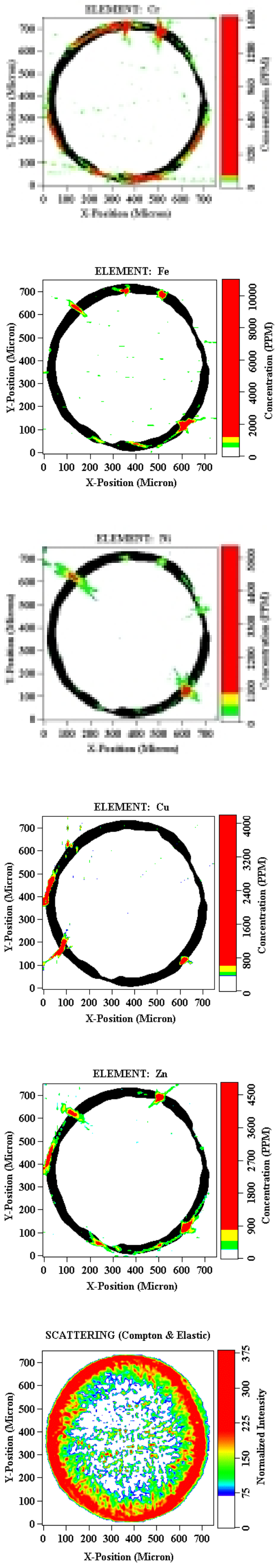

Figure 2 (right): Reconstructed images of the spatial distribution of trace elements with absorption correction.

fluorescence (4.48 keV) can be absorbed by the SiC shell. As a result, the trace elements distributions are most easily detected near the surface of the SiC shell.

The analysis of the images indicates that the spatial distributions of the trace elements are mostly localized at the outer edge of the SiC shell. The reconstructed images imply that a higher counting rate is required to improve the signal-to-noise ratio for low-energy fluorescence lines. The quality of reconstructed images depends also on the selection of a proper number for intensity levels of object/background in the reconstruction routines. At the present time, however, it is not possible to confidently identify the origin of the trace elements; they may have originated from the impurities associated with the fuel, SiC, and/or fabrication processes. Measurements planned for nonirradiated fuel balls will settle this issue.

X-ray microtomography is an emerging technique made practical by high-brilliance x-ray sources, advanced x-ray focusing optics, and high-performance x-ray detectors. We have demonstrated that the fluorescence microtomography technique can be a powerful tool for investigating elemental distributions in materials. The technique is nondestructive and noninvasive with high spatial resolution. It is sensitive to high-Z trace elements in a low-Z matrix with part-per-million accuracy, and has a good signal-to-noise ratio. Fluorescence microtomography can be used to simultaneously identify the elemental distributions of many trace elements. The main drawback of fluorescence microtomography is the slow data collection rate. The results of this experiment point to several ways to greatly accelerate data collection. For example, with a broad-bandpass monochromator, the fluorescence signal can be increased by two to three orders of magnitude with no loss in spatial resolution. This increase in signal will allow three-dimensional maps to be obtained. With such an intense probe, it will, however, be necessary to use wavelength-dispersive spectrometers with integrating rather than single-photon detectors. Such an arrangement will simultaneously increase spatial resolution and will greatly increase the sensitivity for minor trace elements of interest.

It should also be noted that in our experiment, the beam energy was much lower than the K absorption edges of heavy elements such as Cs, Ce, Eu, and Ru. We therefore could not excite the K-lines of these elements. The L-lines are masked by overlapping K-lines of less interesting trace elements. To positively measure the elemental distribution of Cs, for example, either a crystal spectrometer or a high-energy (>36 keV) x-ray probe is required. We intend to try both methods in future measurements.

Acknowledgments

Research was sponsored in part by the LDRD of the Oak Ridge National Laboratory and the Division of Materials Sciences, U.S. Dept. of Energy under Contract DE-AC05-96OR22464 with Lockheed Martin Energy Research Corporation. Experimental measurements were made on beamline 2-ID-D at the Advanced Photon Source, Argonne National Laboratory, which is supported by the U.S. Dept. of Energy, Basic Energy Science, Office of Science, under Contract No. W-31-109-Eng-38.

References

[1] B.F. Myers, F.C. Montgomery, and K.E. Partain, *Doc No. 909055, GA Technologies Inc*., (1986).
[2] P. Krautwasser, G.M. Begun, and P. Angelini, *J. of American Ceramic Society*, **66** 424 (1983).
[3] C.J. Sparks, *Synchrotron Radiation Research*, (Plenum Press, New York, 1980) 459–512.
[4] W. Yun, B. Lai, D. Shu, A. Kounsary, Z. Cai, J. Barraza, and D. Legnini, *Design of a Dedicated Beamline for X-ray Microfocusing and Coherence Based Techniques at the Advanced Photon Source*.
[5] A.C. Huber, J.A. Pantazis, and V. Jordanov, *Nucl. Inst. Meth. B* **99** 665 (1995).
[6] M.O. Krause, C.W. Nestor, Jr., C.J. Sparks, Jr., and E. Ricci, *Oak Ridge National Laboratory Technical Report ORNL-5399*, (1978).
[7] R.H. Huesman, G.T. Gullberg, W.L. Greenberg, and T.F. Budinger, *Lawrence Berkeley Laboratory Publication No. 214, U. of California*, (1977).